AIChE

Effects of Influent Organic Loading Rates and Electrode Locations on the Electrogenesis Capacity of Constructed Wetland-Microbial Fuel Cell Systems

Dan Xu,[a,b] En-Rong Xiao,[b] Peng Xu,[b,c] Yin Zhou,[b,c] Qiao-Hong Zhou,[b] Dong Xu,[b] and Zhen-Bin Wu[b]

[a]College of Resources and Environmental Engineering, Wuhan University of Technology, Wuhan 430070, People's Republic of China

[b]State Key Laboratory of Freshwater Ecology and Biotechnology, Institute of Hydrobiology, Chinese Academy of Sciences, Wuhan 430072, People's Republic of China; erxiao@ihb.ac.cn (or) wuzb@ihb.ac.cn (for correspondence)

[c]Graduate University of Chinese Academy of Sciences, Beijing, 100039, China

Published online 5 October 2016 in Wiley Online Library (wileyonlinelibrary.com). DOI 10.1002/ep.12481

Three novel constructed wetland-microbial fuel cells (CW-MFCs), based on electrode location, were developed for wastewater treatment and sustainable electricity production by embedding a MFC into a CW system. In the three CW-MFCs, electrodes were placed in different locations, including bottom anode-rhizosphere cathode CW-MFC (BA-RC-CW-MFC), rhizosphere anode-air cathode CW-MFC (RA-AC-CW-MFC), and bottom anode-air cathode CW-MFC (BA-AC-CW-MFC), to investigate the combined effects of organic loading rates (OLRs) and reactor configurations on the electrogenesis capacity of the hybrid system. All the systems operated continuously to treat five types of synthetic wastewater with increasing OLRs: 9.2, 18.4, 27.6, 55.2, and 92.0 g chemical oxygen demand (COD) m^{-2} d^{-1}. The BA-RC-CW-MFC failed to produce electricity at any OLR, whereas the maximum power densities of 0.79 ± 0.01 and 10.77 ± 0.52 mW m^{-2} were achieved in the RA-AC-CW-MFC with 18.4 g COD m^{-2} d^{-1} influent OLR and in the BA-AC-CW-MFC with 27.6 g COD m^{-2} d^{-1} influent OLR, respectively. The coulombic efficiencies of the RA-AC-CW-MFC and BA-AC-CW-MFC decreased gradually with the increase in influent OLRs.

Keywords: constructed wetland, microbial fuel cell, power density, electrode location, Canna indica var. flava

INTRODUCTION

Microbial fuel cells (MFCs) have garnered much attention recently, owing to their ability to treat wastewater and simultaneously recover energy from wastewaters containing organic matters [1]. In a typical MFC, electrochemically active bacteria growing at the anode act as a catalyst to oxidize organics in wastewater, producing electrons that are transferred to the anode and then flow to the cathode through an external circuit. Electrons arriving at the cathode combine with a reducible compound (e.g., oxygen, nitrate, or sulfate), whereas protons migrate from the anode across a separator, resulting in the generation of electric current [2,3].

To ensure their practical and economical suitability in large-scale applications, much effort has been made to improve the performance and reduce the construction and operating costs of MFCs [4,5]. Incorporating MFCs with traditional constructed wetlands (CWs) is one of the approaches taken towards this goal [6,7]. A CW that involves wetland vegetation, soils, and the associated microbial metabolisms is widely utilized as a cost-effective, efficient wastewater treatment system because of its low operating and maintenance costs and high removal capacity for pollutants [8].

The CW zonation of the redox gradient (−400 − +800 mV) in the vertical direction with depth [9], or in the radial direction around roots [10], makes it possible to embed a MFC into a CW. The combination of CW-MFC has many benefits [11]: (1) it helps improve electricity generation, owing to the greater quantity of organic compounds (electron donors) for anode oxidation; (2) it enhances the removal of some recalcitrant compounds present in wastewater; and (3) the generated electricity may be applied to offset energy consumption by the CW or to power sensors for continuous and automatic monitoring of the CW. Previous research has suggested that power generation varied in proportion to wastewater strength (represented as chemical oxygen demand, COD) and that substrate oxidation was essential for electricity generation [12,13]. Improving the power density not only helps recycle more electrical energy from the wastewater, but also may promote the removal of contaminants. However, the value is still low (<60 mW m^{-2}) [14], and in consequence much effort has been made to improve the system output of CW-MFCs, including optimization of flow regimes, influent COD concentrations, and electrode materials and configurations [6,14–17].

In a conventional MFC, the anode chamber can use organic matter to produce oxidation reactions under anaerobic conditions created by sealing the device and adding nitrogen; whereas the cathode chamber can use oxygen to produce reduction reactions under aerobic conditions created by exposure to the atmosphere. Similarly, when building a CW-MFC, the cathode can be placed in the aerobic environment at the uppermost layer, and the anode can be

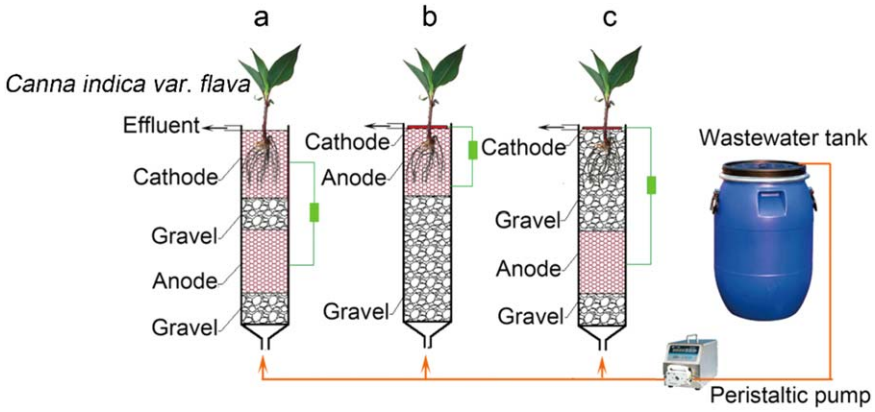

Figure 1. Schematic representation of the three CW-MFCs. (a): BA-RC-CW-MFC; (b): RA-AC-CW-MFC; (c): BA-AC-CW-MFC. [Color figure can be viewed at **wileyonlinelibrary.com**]

placed in the anaerobic environment at the bottom or mid depth of the wetland [14–17].

Furthermore, the presence of plants, which can release oxygen as well as carbon-containing compounds into the rhizosphere in waterlogged soils and flood-prone environments through the aerenchyma and roots [18,19], offers more possible reactor configurations of the CW-MFCs via different electrode locations. The rhizosphere can be a cathode by using oxygen released from the roots as an electron acceptor or an anode by utilizing root exudates of plants as fuel for harnessing bioelectricity [20–22]. Liu *et al*. [14] compared two types of CW-MFCs (with *Ipomoea aquatic* plants in the anodic and cathodic zones) and concluded that the CW-MFC with the anode located in the rhizosphere was appropriate for treating low concentration organic wastewater (COD < 250 mg L^{-1}), whereas the other CW-MFC had the ability to resist high concentrations of organic matter. Furthermore, a maximum power density of 44.63 mW m^{-2} was obtained by placing the cathode around the plant roots [14]. However, the power output with the cathode located around the roots of *Phragmites australis* or *Typha latifolia* is relatively low [23,24]. These significantly different results obtained through utilizing the root as the cathode may be caused by the variation in plant species, which lead to discrepancies in root morphological and structural features, as well as the secretory capacities of oxygen and organics. The suitability of the rhizosphere as the cathode is not well understood yet. Furthermore, due to the discrepancies in the influent conditions, inoculums, matrix, and plants, as well as other parameters, it is difficult to compare the power densities of the CW-MFCs that appear in different reports. The comparative performance, in terms of electricity generation, of these three types of CW-MFC structures under the same conditions remains to be investigated.

To further improve the electricity production capability of the CW-MFC hybrid system, and to optimize its reactor structure, three different electrode placement configurations in continuous up-flow CW-MFCs, including bottom anode-rhizosphere cathode CW-MFC (BA-RC-CW-MFC), rhizosphere anode-air cathode CW-MFC (RA-AC-CW-MFC), and bottom anode-air cathode CW-MFC (BA-AC-CW-MFC), were developed. Additionally, the effect of reactor structure on power output is closely related to influent organic loading rates (OLRs). Thus, the effects of influent OLRs on the power output of the three CW-MFCs were compared.

MATERIALS AND METHODS

CW-MFCs Configuration and Setup

All three types of CW-MFCs (each in triplicate; Figure 1) were composed of a polyvinyl chloride (PVC) column (700 mm height, 160 mm in diameter), a holding bucket (60 L), and a multichannel peristaltic pump (feeding the inflow) connected to an inlet pipe at the bottom of the systems in a room with relatively stable temperature (25 – 30°C). A PVC pipe (700 mm height, 20 mm in diameter) with small holes in the sides wrapped in nylon mesh was inserted vertically into the bottom of each reactor to monitor dissolved oxygen (DO) concentration. Granule active carbon (diameter 3–5 mm) was used as the anode in all the CW-MFCs and as the cathode in the BA-RC-CW-MFC, whereas graphite felts (140 mm external diameter × 70 mm inner diameter × 6 mm thickness) were used as the cathode in the other MFCs. Stainless steel mesh (thickness of 1 mm, 12-mesh), with a working surface area of 493 cm^2, was inserted into the randomly packed granule active carbon to collect the generated electrons efficiently. All graphite components were pretreated by washing them in 1 N HCl and 1 N NaOH to remove possible metal and biomass contamination [3]. The electrodes were connected to an external resistance of 500 Ω by titanium wire (1 mm thickness) to close the electric circuit.

Reactor configurations of the three CW-MFCs, including BA-RC-CW-MFC (Figure 1a), RA-AC-CW-MFC (Figure 1b), and BA-AC-CW-MFC (Figure 1c), are shown in Figure 1. All the systems were planted with equal amounts of freshly developing shoots and rhizomes of *Canna indica* var. *flava*. In the BA-RC-CW-MFC, four layers existed from the bottom upward: the bottom gravel (particle size of 4–8 mm) layer (depth of 100 mm), the anode compartment placed above the gravel (depth of 200 mm), the middle gravel layer (depth of 100 mm), and, at the top, the cathode compartment (depth of 230 mm). The RA-AC-CW-MFC was constructed with a bottom gravel layer (depth of 400 mm), the anode region located around the plant root (depth of 200 mm), and a gravel layer (depth of 24 mm), above which graphite felt as the cathode was placed at the air-water interface. In the BA-AC-CW-MFC, the anode compartment followed the same arrangement and materials used as outlined for the BA-RC-CW-MFC, the cathode setup was the same as the RA-AC-CW-MFC, and a middle gravel layer (depth of 324 mm) was placed between the anode and cathode regions.

Experimental Inoculation and Operation

To start up the CW-MFCs, the anode chamber was inoculated with anaerobic activated sludge (30% v/v) collected from a local domestic wastewater treatment plant (Wuchang Zone, Wuhan, China) and filled with a synthetic wastewater (COD = 150 mg L^{-1}), whereas the cathode was immersed in aerobic activated sludge for 48 h before being introduced to

the device. The synthetic wastewater contained 0.197 g L^{-1} CH_3COONa, 2.307 g L^{-1} $Na_2HPO_4{\cdot}12H_2O$, 0.554g L^{-1} $NaH_2PO_4{\cdot}2H_2O$, 0.191 g L^{-1} NH_4Cl, 0.5 g L^{-1} NaCl, 0.0068 g L^{-1} $CaCl_2{\cdot}6H_20$, 0.1 g L^{-1} $MgSO_4{\cdot}7H_2O$, and 1 g L^{-1} $NaHCO_3$. The systems were operated in batch mode during the enrichment stage. After obtaining stable performances in batch mode, the CW-MFCs were converted to continuous-flow mode with a flow rate of 2.57 mL min^{-1}, giving an HRT of 24 h. In continuous-flow mode, the OLR of the synthetic wastewater was varied from 9.2 to 92.0 g COD m^{-2} d^{-1} by adjusting the influent COD concentration from 50 to 500 mg L^{-1}. The reactors were operated for 3–5 days at each OLR.

Sampling, Analytics, and Calculations

Samples were collected weekly, before quasi-steady-state conditions were achieved. The reactor was assumed to achieve a steady state if voltage values did not vary more than 10% in two consecutive weeks. Once the systems reached steady state, a series of experiments was performed to study the effects of OLR on the energy production of the three CW-MFCs.

The ability of the different reactor configurations to affect electricity generation performance was examined in terms of voltage output and power density. The cell potential (mV) across the external resistors in the CW-MFCs was monitored continuously at 5 min intervals using an on-line data logger (Jisheng R6016/U, Shanghai, China) and current (I) was calculated using Ohm's Law. The current density was calculated by dividing the current by the anodic surface area (mA m^{-2}). To obtain polarization curves at a steady state, the external resistance was changed in a stepwise manner every 15 min (from 50,000 to 5 Ω). The coulombic efficiency (CE) of the systems was determined using Eq. (1) for MFCs under continuous flow [25].

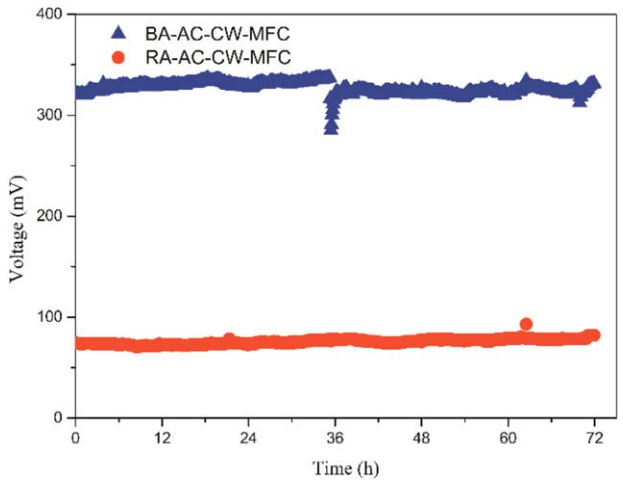

Figure 2. Representative voltage output in different CW-MFCs under 27.6 g COD·m^{-2} d^{-1} OLR. [Color figure can be viewed at **wileyonlinelibrary.com**]

$$CE = \frac{MI}{FqbΔCOD} \quad (1)$$

where CE is coulombic efficiency (%), M is the molecular weight of O_2 (g O_2 mol^{-1} O_2^{-1}; = 32), I is current (mA), F is Faraday's constant (94,685 C mol^{-1}), q is the volumetric influent flow rate (L s^{-1}), b is the number of electrons exchanged per mole of oxygen (mol e^- mol^{-1} O_2^{-1}; = 4), and ΔCOD represents the change in COD between influent and effluent.

RESULTS AND DISCUSSION

Effect of Electrode Locations on Electricity Production

The CW-MFCs were fed at an OLR of 27.6 g COD m^{-2} d^{-1} and flow rate of 2.57 mL min^{-1} during operation of start-up. After approximately a month of operation, the systems achieved constant electricity production. The results of voltage output across a 500 Ω external resistor taken on three consecutive days during steady state are shown in Figure 2. The BA-RC-CW-MFC did not produce electricity during operation (data not shown), whereas average voltages of 73 ± 25 and 329 ± 16 mV were achieved by RA-AC-CW-MFC and BA-AC-CW-MFC, respectively, under 27.6 g COD m^{-2} d^{-1} OLR. Different electricity generations by the BA-AC-CW-MFC and RA-AC-CW-MFC reported here could be attributed to the different anode locations in the MFCs. The reason there was no voltage generation in the BA-RC-CW-MFC was probably that limited available oxygen in the cathode region was present. In some previous studies of planted-MFCs (PMFCs) [22] or CW-MFCs [6], the excreted oxygen from plant roots that had high amounts of aerenchyma could function efficiently as a cathodic electron acceptor when the cathode was placed in an aerobic rhizosphere. However, quite low voltage generation was obtained in other studies, which also used roots as the cathode region [23,24]. Two possible reasons exist for that the cathode located in the wetland plants root could not work efficiently or even stopped working: a limited capacity to release oxygen through the aerenchyma of wetland plants and a high concentration of organic matter flowing into the cathode area [6]. For the BA-RC-CW-MFC, the restrictive oxygen excreted via the root of wetland plants may be the primary reason for electricity production failure. The DO in the cathode region of the BA-RC-CW-MFC was 0.45 mg L^{-1} (Table 1), which is significantly lower than the normal value of such in other CW-MFCs with the cathode located in the rhizosphere [16,26]. A comparison of studies regarding the performances of various PMFCs or CW-MFCs related to living plants was compiled and is presented in Table 2. Living plants can use root exudates, which are oxidized at the anode, or employ a rhizosphere biocathode, which acts as an electron acceptor and concurrently reduces H^+ to H_2O. The roots of some plants, such as rice plants, *Canna indica*, and *Ipomoea aquatic*, can be used as both an anode and a cathode (Table 2), which may be due to the different operational conditions. Root depth and the secretory abilities of oxygen and organic matter via the roots

Table 1. Comparative performance of different systems under 27.6 g COD·m^{-2} d^{-1} OLR.

System	Anode		Cathode		Average voltage (mV)	Average power density (mW m^{-2})
	Depth (mm)	DO (mg L^{-1})	Depth (mm)	DO (mg L^{-1})		
BA-RC-CW-MFC	100–300	0.21	400-630	0.45	0	0
RA-AC-CW-MFC	400–600	0.13	624-630	0.55	73 ± 25	0.53 ± 0.18
BA-AC-CW-MFC	100–300	0.30	624-630	2.38	329 ± 16	10.77± 0.52

Table 2. Living plants used in the previous PMFC or CW-MFC studies.

Plant	Function	MFC configuration	Feed (mg L^{-1})	Maximum power density (mWm^{-2})	Ref.
Rice plants	Assisting the anode	Single-chamber PMFC	–	6	[28]
		Single-chamber PMFC	–	26	[21]
		Single-chamber PMFC	–	3.52–14.44	[29]
	Assisting the cathode	Single-chamber PMFC	–	201	[22]
		Single-chamber PMFC			
Spartina anglica	Assisting the anode	Dual-chamber PMFC	–	100	[30]
		Dual-chamber PMFC	–	211	[31]
		Single-chamber PMFC	–	222	[32]
Canna indica	Assisting the anode	Single-chamber PMFC	–	18	[33]
	Assisting the cathode	Vertical subsurface flow CW-MFC	Sucrose (8000) and methylene blue dye (500–2000)	15.73	[34]
		Vertical subsurface flow CW-MFC	Glucose (250–750)	<0.05 W m^{-3}	[17]
Ipomoea aquatica	Assisting the anode	Vertical subsurface flow CW-MFC	50–1000	13.94–39.07	[14]
	Assisting the cathode	Vertical subsurface flow CW-MFC	COD (180) and ABRX3 (18)	0.455 W m^{-3}	[35]
		Vertical subsurface flow CW-MFC	Glucose (600) and X-3B artificial wastewater (180)	0.302 W m^{-3}	[36]
		Vertical subsurface flow CW-MFC	193–205	12.42	[26]
		Vertical subsurface flow CW-MFC	~200	55.05	[14]
Phragmites australis	Assisting the cathode	Horizontal subsurface flow CW-MFC	250, 560, 1100	0.15, 43, stop working	[6]
		Simultaneous upflow–downflow CW-MFC	583	0.276 W m^{-3}	[37]
		Vertical subsurface flow CW-MFC	411–854	0.268 W m^{-3}	[16]
		Vertical subsurface flow CW-MFC	455–3220	9.35 (with aeration)	[23]
Arundinella anomala	Assisting the anode	Single-chamber PMFC	–	22	[32]
Glyceria maxima	Assisting the anode	Dual-chamber PMFC	–	72	[38]
Pennisetum setaceum	Assisting the anode	Single-chamber PMFC	–	163	[39]
Typha latifolia	Assisting the cathode	Vertical subsurface flow CW-MFC	~315	6.12 (with aeration)	[24]

may also have an important influence on the selection of the root as an anode or a cathode, which should be studied further. Higher voltage output was achieved by the BA-AC-CW-MFC compared with the RA-AC-CW-MFC. Possible reasons for this result are as follows: (1) there are more available substrates in the anode of the BA-AC-CW-MFC, because its anode region is closer to the inlet, and (2) it is possible that untreated organic matter and root exudation in the anodic region flowed to the cathodic region in the RA-AC-CW-MFC, because of the short distance (24 mm) between the anode and the cathode.

Polarization curves were obtained to determine the maximum power generation and internal resistance in the RA-AC-CW-MFC and BA-AC-CW-MFC (Figure 3). The BA-AC-CW-MFC exhibited a maximum power density of 11.21 mW m^{-2}, which was almost tenfold higher than the 1.05 mW m^{-2} achieved in the RA-AC-CW-MFC. A polarization curve can provide information about major losses that are decisive for the fuel cell performance [27]: (1) activation-related losses caused by sluggish electrode kinetics of the electrochemical reactions at the electrodes; (2) ohmic losses governed by resistance to the flow of ions in the electrolyte and resistance to flow of electrons through the electrode, which are proportional to the current density; and (3) mass-transport-related losses caused by finite mass transport limitation rates of the reactants and that depend strongly on the current density, reactant activity, and electrode structure. As seen in Figure 3, the decrease in the voltage outputs of the two CW-MFCs along with the decrease in the external resistors indicated existing ohmic losses. Moreover, the ohmic resistances of the RA-AC-CW-MFC and BA-AC-CW-MFC were 188 and 319 Ω, respectively. These results suggest that the decrease of the space between the anode and the cathode may have reduced the ohmic internal resistance. However, uncompleted oxidization of the organics in the anodic region flowed to the cathodic one in RA-AC-CW-MFC and reduced the output voltage. Thus, optimizing electrode spacing is crucial for electricity generation by CW-MFCs, and depends on influent OLR, HRT, DO, redox potential, etc.

Combined Effects of Influent OLRs and Electrode Locations on Electricity Production

After the systems reached stable performance, the OLR of the synthetic wastewater was varied from 9.2 to 92.0 g COD m^{-2} d^{-1} by adjusting the influent COD concentration from 50 to 500 mg L^{-1}. Voltage output and current density varied

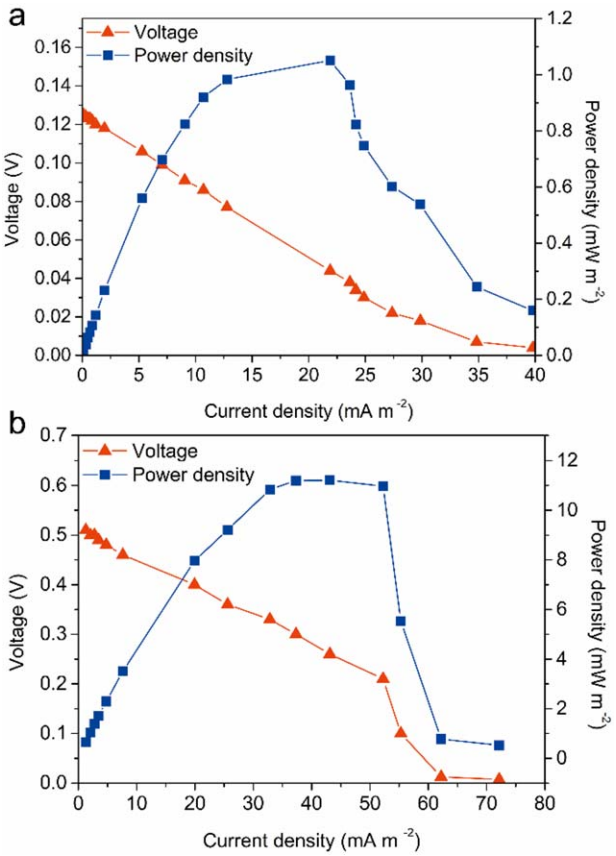

Figure 3. Cell polarization and power density curves RA-AC-CW-MFC (a) and BA-AC-CW-MFC (b) under 27.6 g COD·m^{-2} d^{-1} OLR. [Color figure can be viewed at **wileyonlinelibrary.com**]

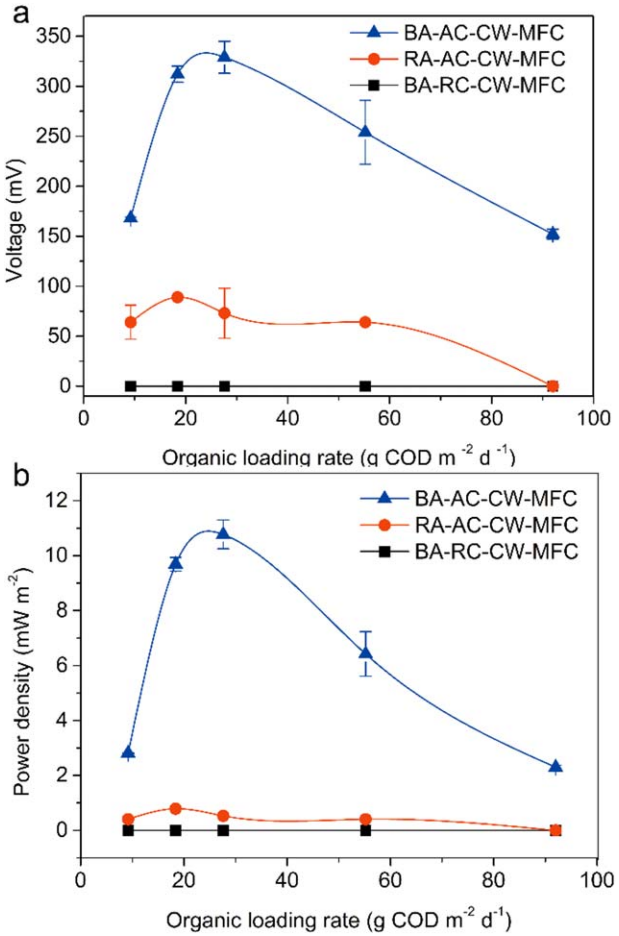

Figure 4. Voltage output (a) and power density (b) of CW-MFCs with different OLRs. [Color figure can be viewed at **wileyonlinelibrary.com**]

with different OLRs (Figure 4). According to Figure 4, both voltage output and current density of the RA-AC-CW-MFC and BA-AC-CW-MFC showed similar variation tendencies. However, the BA-RC-CW-MFC failed to produce electricity at any OLR, which further confirmed the restrictive oxygen excreted through the plant roots is the primary limiting factor for electricity generation failure. The power density of the BA-AC-CW-MFC was 2.81 ± 0.02 and 9.69 ± 0.25 mW m^{-2} at the concentrations of 9.2 and 18.4 g COD m^{-2} d^{-1} influent OLR, respectively, whereas the power density of the RA-AC-CW-MFC was 0.41 ± 0.11 and 0.79 ± 0.01 mW m^{-2} at the same concentrations. The maximum power densities of 0.79 ± 0.01 and 10.77 ± 0.52 mW m^{-2} were achieved in the RA-AC-CW-MFC with 18.4 g COD m^{-2} d^{-1} influent OLR and in the BA-AC-CW-MFC with 27.6 g COD m^{-2} d^{-1} influent OLR, respectively. However, when the OLRs were raised higher than 18.4 g COD m^{-2} d^{-1} influent OLRs in the RA-AC-CW-MFC and 27.6 g COD m^{-2} d^{-1} influent OLRs in the BA-AC-CW-MFC, the voltage outputs and power densities of the two systems decreased gradually. When the OLR was increased to 92.0 g COD m^{-2} d^{-1}, the RA-AC-CW-MFC even stopped working, whereas the minimum power density of 2.30 ± 0.08 mW m^{-2} was achieved in the BA-AC-CW-MFC. In addition, the voltage output and power density of the BA-AC-CW-MFC were higher than those of the RA-AC-CW-MFC were at any OLR. Moreover, the discrepancies in the voltage outputs and power densities between the two systems reached a minimum value at the minimum OLR of 9.2 g

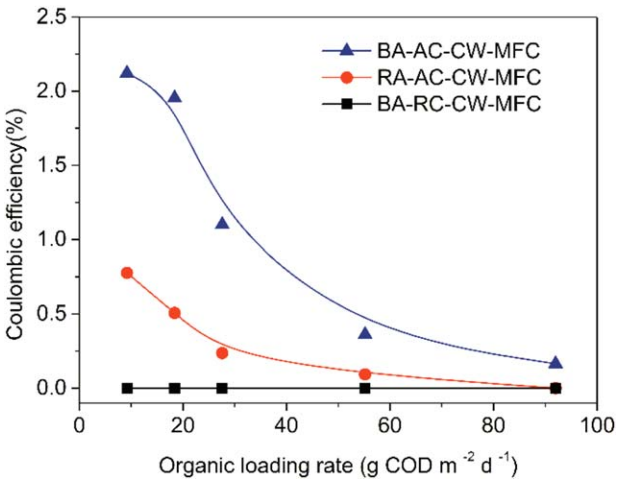

Figure 5. CE of CW-MFCs varied with influent OLRs. [Color figure can be viewed at **wileyonlinelibrary.com**]

COD m^{-2} d^{-1}. These results indicate that the RA-AC-CW-MFC is more suitable for treating influent with a low OLR, whereas the BA-AC-CW-MFC shows a higher electrogenesis

capacity for influents with a wide range of OLRs. Similar results have been reported [14].

The CEs of all the CW-MFC systems varied with influent OLRs, as shown in Figure 5. The BA-AC-CW-MFC achieved CEs in the range of 0.16–2.12%, which were higher than those of the RA-AC-CW-MFC in the range of 0–0.78%. The low CEs indicate that the majority of organic matter was removed by methanogens or other microbes, instead of by the anodophilic bacteria. The CEs of the BA-AC-CW-MFC declined with increased influent OLR, which is consistent with the results of previous studies on CW-MFCs [16,17]. Comprehensive considerations of the material and configuration of the reactor, type and concentration of the feed, operating mode (batch or continuous), wetland plant species, and hydraulic retention time, etc., are necessary to acquire optimal CEs and power densities.

CONCLUSION

In this study, the combined effects of influent OLR and electrode location on the power output in continuous upflow CW-MFCs were investigated. When placing the cathode in the rhizosphere, the CW-MFC planted with *Canna indica* var. *flava* failed to produce electricity because of the limited capacity of oxygen release through the aerenchyma. Higher voltage output and power generation were achieved by placing the cathode in the air-water interface in comparison with the cathode in the rhizosphere. Moreover, the maximum power densities achieved in the RA-AC-CW-MFC and BA-AC-CW-MFC were 18.4 and 27.6 g COD m^{-2} d^{-1} influent OLR, respectively. The RA-AC-CW-MFC was more suitable for treating influent with a low OLR, whereas the BA-AC-CW-MFC showed a higher electrogenesis capacity for influents with a wide range of OLRs. Nevertheless, when choosing a wetland plant as an anode or a cathode, its root depths and secretory abilities of oxygen and organic matter under different operational conditions need to be studied further. To acquire optimal CE and power density, comprehensive considerations for reactor architectures and operational conditions are critical.

ACKNOWLEDGMENTS

This research was supported financially by the National Natural Science Foundation of China (51308530), the Natural Science Foundation of Hubei Province (2015CFB558) and the Key Research Program of the Chinese Academy of Sciences (KFZD-SW-302-02).

LITERATURE CITED

1. Du, Z.W., Li, H.R., & Gu, T.K. (2007). A state of the art review on microbial fuel cells: A promising technology for wastewater treatment and bioenergy, Biotechnology Advances, 25, 464–482.
2. Rabaey, K., & Verstraete, W. (2005). Microbial fuel cells: Novel biotechnology for energy generation, Trends in Biotechnology, 23, 291–298.
3. Bond, D.R., & Lovley, D.R. (2003). Electricity production by Geobacter sulfurreducens attached to electrodes, Applied and Environmental Microbiology, 69, 1548–1555.
4. Wei, J.C., Liang, P., & Huang, X. (2011). Recent progress in electrodes for microbial fuel cells, Bioresource Technology, 102, 9335–9344.
5. Elangovan, M., & Dharmalingam, S. (2016). Scaleup suitability of sulfonated polyether ether ketone membrane-based microbial fuel cell, Environmental Progress & Sustainable Energy, 35, 80–87.
6. Villasenor, J., Capilla, P., Rodrigo, M.A., Canizares, P., & Fernandez, F. (2013). Operation of a horizontal subsurface flow constructed wetland-microbial fuel cell treating wastewater under different organic loading rates, Water Research, 47, 6731–6738.
7. Doherty, L., Zhao, Y.Q., Zhao, X.H., Hu, Y.S., Hao, X.D., Xu, L., & Liu, R.B. (2015). A review of a recently emerged technology: Constructed wetland - Microbial fuel cells, Water Research, 85, 38–45.
8. Vymazal, J. (2007). Removal of nutrients in various types of constructed wetlands, Science of the Total Environment, 380, 48–65.
9. Corbella, C., Garfí, M., & Puigagut, J. (2014). Vertical redox profiles in treatment wetlands as function of hydraulic regime and macrophytes presence: Surveying the optimal scenario for microbial fuel cell implementation, Science of the Total Environment, 470, 754–758.
10. Bezbaruah, A.N., & Zhang, T.C. (2004). pH, redox, and oxygen microprofiles in rhizosphere of bulrush (*Scirpus validus*) in a constructed wetland treating municipal wastewater, Biotechnology and Bioengineering, 88, 60–70.
11. Xu, B.J., Ge, Z., & He, Z. (2015). Sediment microbial fuel cells for wastewater treatment: Challenges and opportunities, Environmental Science: Water Research and Technology, 1, 279–284.
12. Logan, B.E. (2005). Simultaneous wastewater treatment and biological electricity generation, Water Science and Technology, 52, 31–37.
13. He, Z., Minteer, S.D., & Angenent, L.T. (2005). Electricity generation from artificial wastewater using an upflow microbial fuel cell, Environmental Science and Technology, 39, 5262–5267.
14. Liu, S.T., Song, H.L., Wei, S.Z., Yang, F., & Li, X.N. (2014). Bio-cathode materials evaluation and configuration optimization for power output of vertical subsurface flow constructed wetland - microbial fuel cell systems, Bioresource Technology, 166, 575–583.
15. Wu, D., Yang, L.Y., Gan, L., Chen, Q., Li, L., Chen, X., Wang, X., Guo, L.Y., & Miao, A.J. (2015). Potential of novel wastewater treatment system featuring microbial fuel cell to generate electricity and remove pollutants, Ecological Engineering, 84, 624–631.
16. Doherty, L., Zhao, X.H., Zhao, Y.Q., & Wang, W.K. (2015). The effects of electrode spacing and flow direction on the performance of microbial fuel cell-constructed wetland, Ecological Engineering, 79, 8–14.
17. Srivastava, P., Yadav, A.K., & Mishra, B.K. (2015). The effects of microbial fuel cell integration into constructed wetland on the performance of constructed wetland, Bioresource Technology, 195, 223–230.
18. Colmer, T. (2003). Long-distance transport of gases in plants: a perspective on internal aeration and radial oxygen loss from roots, Plant, Cell and Environment, 26, 17–36.
19. Rovira, A.D. (1969). Plant root exudates, The Botanical Review, 35, 35–57.
20. Deng, H., Chen, Z., & Zhao, F. (2012). Energy from plants and microorganisms: progress in plant–microbial fuel cells, ChemSusChem, 5, 1006–1011.
21. Schamphelaire, L.D., Bossche, L.V.D., Dang, H.S., Höfte, M., Boon, N., Rabaey, K., & Verstraete, W. (2008). Microbial fuel cells generating electricity from rhizodeposits of rice plants, Environmental Science and Technology, 42, 3053–3058.
22. Chen, Z., Huang, Y.C., Liang, J.H., Zhao, F., & Zhu, Y.G. (2012). A novel sediment microbial fuel cell with a biocathode in the rice rhizosphere, Bioresource Technology, 108, 55–59.
23. Zhao, Y.Q., Collum, S., Phelan, M., Goodbody, T., Doherty, L., & Hu, Y.S. (2013). Preliminary investigation of constructed wetland incorporating microbial fuel cell:

Batch and continuous flow trials, Chemical Engineering Journal, 229, 364–370.
24. Oon, Y.L., Ong, S.A., Ho, L.N., Wong, Y.S., Oon, Y.S., Lehl, H.K., & Thung, W.E. (2015). Hybrid system up-flow constructed wetland integrated with microbial fuel cell for simultaneous wastewater treatment and electricity generation, Bioresource Technology, 186, 270–275.
25. Logan, B.E., Hamelers, B., Rozendal, R., Schröder, U., Keller, J., Freguia, S., Aelterman, P., Verstraete, W., & Rabaey, K. (2006). Microbial fuel cells: Methodology and technology, Environmental Science and Technology, 40, 5181–5192.
26. Liu, S.T., Song, H.L., Li, X.N., & Yang, F. (2013). Power generation enhancement by utilizing plant photosynthate in microbial fuel cell coupled constructed wetland system, International Journal of Photoenergy, 2013, 1–10.
27. Appleby, A.J., & Foulkes, F.R. (1988). Fuel Cell Handbook, New York: Van Nostrand Reinhold, Co. Inc.
28. Kaku, N., Yonezawa, N., Kodama, Y., & Watanabe, K. (2008). Plant/microbe cooperation for electricity generation in a rice paddy field, Applied Microbiology and Biotechnology, 79, 43–49.
29. Takanezawa, K., Nishio, K., Kato, S., Hashimoto, K., & Watanabe, K. (2010). Factors affecting electric output from rice-paddy microbial fuel cells, Bioscience, Biotechnology, and Biochemistry, 74, 1271–1273.
30. Timmers, R.A., Strik, D.P., Hamelers, H.V., & Buisman, C.J. (2010). Long-term performance of a plant microbial fuel cell with *Spartina anglica*, Applied Microbiology and Biotechnology, 86, 973–981.
31. Helder, M., Strik, D., Hamelers, H., Kuijken, R., & Buisman, C. (2012). New plant-growth medium for increased power output of the plant-microbial fuel cell, Bioresource Technology, 104, 417–423.
32. Helder, M., Strik, D., Hamelers, H., Kuhn, A., Blok, C., & Buisman, C. (2010). Concurrent bio-electricity and biomass production in three Plant-Microbial Fuel Cells using *Spartina anglica*, *Arundinella anomala* and *Arundo donax*, Bioresource Technology, 101, 3541–3547.
33. Lu, L., Xing, D.F., & Ren, Z.J. (2015). Microbial community structure accompanied with electricity production in a constructed wetland plant microbial fuel cell, Bioresource Technology, 195, 115–121.
34. Yadav, A.K., Dash, P., Mohanty, A., Abbassi, R., & Mishra, B.K. (2012). Performance assessment of innovative constructed wetland-microbial fuel cell for electricity production and dye removal, Ecological Engineering, 47, 126–131.
35. Fang, Z., Song, H.L., Cang, N., & Li, X.N. (2015). Electricity production from Azo dye wastewater using a microbial fuel cell coupled constructed wetland operating under different operating conditions, Biosensors and Bioelectronics, 68, 135–141.
36. Fang, Z., Song, H.L., Cang, N., & Li, X.N. (2013). Performance of microbial fuel cell coupled constructed wetland system for decolorization of azo dye and bioelectricity generation, Bioresource Technology, 144, 165–171.
37. Doherty, L., & Zhao, Y.Q. (2015). Operating a two-stage microbial fuel cell–constructed wetland for fuller wastewater treatment and more efficient electricity generation, Water Science and Technology, 72, 421–428.
38. Timmers, R.A., Strik, D.P., Hamelers, H.V., & Buisman, C.J. (2013). Electricity generation by a novel design tubular plant microbial fuel cell, Biomass and Bioenergy, 51, 60–67.
39. Chiranjeevi, P., Mohanakrishna, G., & Mohan, S.V. (2012). Rhizosphere mediated electrogenesis with the function of anode placement for harnessing bioenergy through CO_2 sequestration, Bioresource Technology, 124, 364–370.